Taylor & Francis
Taylor & Francis Group

BRIEF REPORT

✂ OPEN ACCESS ⟳ Check for updates

Early response evaluation of PD-1 blockade in NSCLC patients through FDG-PET-CT and T cell profiling of tumor-draining lymph nodes

Frank J. Borm[a], Jasper Smit[b], Joyce Bakker[c,d,e], Maurits Wondergem[f], Egbert F. Smit[a,b], Adrianus J. de Langen[b], and Tanja D. de Gruijl[c,d,e]

[a]Department of Pulmonary Diseases, Leiden University Medical Centre, Leiden, The Netherlands; [b]Department of Thoracic Oncology, NKI-AvL, Amsterdam, The Netherlands; [c]Amsterdam UMC Location Vrije Universiteit, Medical Oncology, Amsterdam, Netherlands; [d]Cancer Center Amsterdam, Cancer Immunology, Amsterdam, Netherlands; [e]Cancer Immunology, Amsterdam Institute for Infection and Immunology, Amsterdam, Netherlands; [f]Department of Nuclear Medicine, NKI-AvL, Amsterdam, The Netherlands

ABSTRACT

Better biomarkers for programmed death - (ligand) 1 (PD-(L)1) checkpoint blockade in non-small cell lung cancer (NSCLC) are needed. We explored the predictive value of early response evaluation using Fluor-18-deoxyglucose positron emission tomography and pre- and on-treatment flowcytometric T-cell profiling in peripheral blood and tumor-draining lymph nodes (TDLN). The on-treatment evaluation was performed 7–14 days after the start of PD-1 blockade in NSCLC patients. These data were related to (pathological) tumor response, progression-free survival, and overall survival (OS). We found that increases in total lesion glycolysis (TLG) had a strong reverse correlation with OS ($r = -0.93$, $p = 0.022$). Additionally, responders showed decreased progressors and increased Treg frequencies on-treatment. Frequencies of detectable PD-1-expressing CD8$^+$ T cells decreased in responders but remained stable in progressors. This was especially found in the TDLN. Changes in activated Treg rates in TDLN were strongly but, due to low numbers of data points, non-significantly correlated with ΔTLG and reversely correlated with OS.

Introduction

Indications for PD-(L)1 checkpoint inhibitors in non-small cell lung cancer (NSCLC) are still expanding. Several factors are known to be associated with treatment response, including PD-L1 expression on tumor cells and associated leukocytes, infiltrating lymphocyte rates, and tumor mutational burden. However, these biomarkers lack the predictive power to make clear treatment discisions.[1]

Fluor-18-deoxyglucose positron emission tomography (^{18}F-FDG-PET) is a noninvasive and routinely performed procedure that provides data on the glucose metabolism of tumor lesions. The application of a single ^{18}F-FDG-PET before treatment in response prediction has been extensively studied, but there is no clear imaging parameter that outperforms the predictive power of PD-L1 expression on tumor cells.[2] Another approach is performing ^{18}F-FDG-PET at baseline and shortly after treatment initiation to assess the changes in tracer uptake induced by checkpoint inhibitor therapy. For example, in patients with head and neck squamous cell carcinoma (HNSCC) who underwent two cycles of neoadjuvant immunotherapy, an increase in ^{18}F-FDG tumor uptake expressed as total lesion glycolysis (TLG) (at days 21–28) was correlated with unfavorable outcomes.[3]

Another source of potential predictive biomarkers is the tumor-draining lymph node (TDLN). TDLNs are heavily influenced by the tumor, which is illustrated by the observation that TDLNs become immunosuppressive within a week after tumor implantation.[4] This pre-metastatic niche is induced by the tumor through immune modulatory exosomes and soluble mediators. Suppression of dendritic cells, a low CD4/CD8 ratio, and high rates of Tregs have all been related to metastatic spread to TDLNs.[5] Moreover, recent preclinical studies have provided proof that the TDLN is essential for the induction of an effective antitumor response upon the initiation of immune checkpoint inhibitor (ICI) therapy.[5] Its unique immunological properties and its essential role in ICI treatment response make the TDLN a logical site for early response biomarker discovery.

It has been established that endobronchial ultrasound (EBUS)-guided fine-needle aspiration of TDLN, combined with multi-parameter fluorescence-activated cell sorting (FACS), allows for the quantitation and phenotypic profiling of T cells in the TDLN of patients with NSCLC.[6–8] These studies revealed an immunosuppressed microenvironment that is unique for the TDLN and differs from blood or non-tumor-draining lymph nodes (NDLNs). Most notably, in a previous study, we observed higher levels of PD-1 expressed on both activated Tregs and CD4$^+$ or CD8$^+$ T cells in TDLN compared to peripheral blood mononuclear cells (PBMCs) and NDLN.[8]

In this manuscript, we are the first to report pre- and on-treatment sequential measurements of T-cell subsets from the TDLN in NSCLC patients treated with a PD-1 inhibitor (ClinicalTrials.gov Identifier: NCT 04082988, NCT 03446911). In parallel, we performed sequential ^{18}F-FDG PETs to study the changes in tumor FDG uptake in association with the immune monitoring findings. In addition, we determined the association of these dynamics with clinical outcomes and found a possibly predictive early immune response signature that warrants further clinical exploration.

Materials and methods

Patients

Patients with NSCLC, scheduled to undergo PD-1 blockade, were included in this study (Table 1). Participating stage-IV patients had progressed after at least one line of platinum-based doublet chemotherapy prior to receiving systemic nivolumab (NCT 04082988). Early-stage patients were randomized between two cycles of neo-adjuvant pembrolizumab with or without SBRT or SBRT without pembrolizumab before resection and pathological response evaluation (NCT 03446911). EBUS-guided TDLN and blood samples were taken at baseline and 14 days after immunotherapy for flow cytometric analysis. For this analysis, one patient who received pembrolizumab monotherapy was included. Earlier treatment with PD-(L)1 checkpoint inhibitors was not allowed in both studies. The studies were conducted in accordance with the Declaration of Helsinki and were approved by the Institutional Review Board of NKI-AVL in Amsterdam. Prior to inclusion, each patient signed a written informed consent, after receiving verbal and written explanation.

After treatment initiation, advanced-stage patients were evaluated for response with CT; clinical response was defined as a partial response or stable disease according to RECIST 1.1 and a progression-free survival (PFS) longer than 3 months. In the neo-adjuvant setting, response was defined as complete or major (i.e. >90% tumor clearance) pathological response.

All subjects enrolled in NCT 04082988 underwent a whole-body ^{18}F-FDG-PET scan and EBUS with fine needle aspiration (FNA) of the TDLN at baseline. An additional ^{18}F-FDG-PET scan and EBUS were performed between days 7 and 14 after the first treatment cycle. Both studies were unfortunately terminated prematurely, NCT 04082988 as PD-1 blockade became

the first-line treatment and NCT 03446911 as a result of slow accrual.

EBUS-FNA

Needle aspirations were performed with a 22-gauge needle under sedation using midazolam or propofol with or without alfentanil, as previously described. The TDLN was punctured six times consisting of 15 passes to maximize the cell yield. Cells obtained through needle aspirations were collected in a 7.5-ml culture medium and prepared for flow cytometry as previously described.[8] For an overview of EBUS-FNA procedures and cell yields, see Table S2.

Blood sampling

Heparinized blood samples were drawn prior to the endoscopic procedure at baseline and 7–14 days after the first cycle of PD-1 checkpoint inhibitor. PBMCs were isolated and cryopreserved until simultaneous flow cytometric analysis of all pre- and on-treatment samples per patient to avoid inter-assay variability as previously described.[8]

Phenotypic analysis by flow cytometry

PBMC and TDLN single-cell suspensions were washed with FACS buffer (PBS + 0.1% bovine serum albumin [BSA] + 0.02% NaN3). Cells were resuspended in 50 μL of FACS buffer and stained in a total volume of 75 μL for 30 min at 4°C for surface expression using monoclonal antibodies directed against CD3 (PerCP-Cy5.5), CD8 (V500), CD25 (APC), CD127 (BV421), CD45RA (APC-H7), PD-1 (PE-Cy7) (BD Biosciences, San Jose, CA, USA), LAG-3 (PE-Cy7) (eBioscience, San Diego, CA, USA), CD4 (AF700), and TIM-3 (BV421) (Biolegend, San Diego, CA, USA) pre-diluted in Brilliant-violet staining buffer (BD Biosciences). Cells were washed with cold PBS, fixed, and permeabilised using the eBioscience FoxP3 staining kit according to the manufacturer's instructions. Antibodies against FoxP3 (PE) (eBioscience, San Diego, CA, and USA), Ki-67 (FITC), and CTLA-4 (BD Biosciences) were used for intracellular staining and incubated for 30 min at 4°C. Stained cells were analyzed on a BD LSR Fortessa X-20 flow cytometer, and data were analyzed using Kaluza analysis software (Beckman Coulter, Brea, CA, USA).

Table 1. Patient characteristics and study procedures.

Patient	Stage	Pathology	PD-L1 TPS (%)	BOR	PES	OS	EBUS^{α}	FDG PETα (y/n)
1	cTxN3M0	Adenocarcinoma	<1	PR	191	303	n	n
2	cT3N3M0	Adenocarcinoma	20	PR	167	430	y	y
3	cT4N3M1c	NOS	10	PD	37	37	n	n
4	-	-	-	-	-	-	-	-
5	cT3N3M1c	Adenocarcinoma	<1	SD	84	276	y	y
6	cT1cN3M1c	Adenocarcinoma	<1	PD	52	95	y	y
7	cT2N3M1c	Adenocarcinoma	30	PD	56	90	y	y
8	cT4N3M1a	Squamous	<1	PD	16	16	n	n
9	cT4N2N0	Squamous	<1	SD	107	107	n	y
10	cT2aN0M0	Adenocarcinoma	NA	cPR	-	-	y	n

Patients 1–9 were treated with second-line and beyond nivolumab (ClinicalTrials.gov Identifier: NCT04082988). Patient 10: patient with early-stage NSCLC. Lobectomy and systematic lymph node dissection were performed after two cycles of neoadjuvant pembrolizumab (ClinicalTrials.gov Identifier: NCT03446911). PR: partial response; SD: stable disease; cPR: complete pathological response; NA: not available; BOR: best observed response; PFS: progression-free survival; OS: overall survival; TPS: tumor proportion score.
α: at baseline and on-treatment.

^{18}F-FDG-PET

^{18}F-FDG-PET was performed at baseline (<4 weeks before the start of treatment) and 7–14 days after the treatment initiation with nivolumab. Primary tumor and metastatic lesions were identified and segmented on all ^{18}F-FDG-PET images using in-house developed software[9]. Volumes of interest (VOI) were delineated over the entire tumor lesions. Tracer uptake in all delineated VOIs was semi-quantitatively assessed as a standardized uptake value (SUV). SUVpeak all and hottest lesion, SUVmax all and hottest lesion, and TLG were reported. On-treatment obtained ^{18}F-FDG-PET tracer uptake was compared to baseline.

Statistical analysis

This was an explorative study with limited numbers of studied patients and samples, and the obtained data should be interpreted with caution and regarded as hypothesis generating. A Pearson correlation test was performed on the PET data, clinical outcome, and immune subsets.

Results

Patient characteristics

In total, 10 patients were originally included in this pilot study (Table S1). Four out of 10 underwent all study procedures (patients 2, 5, 6, and 7). Patients 1, 3, 4, and 8 detoriated quickly and did not undergo the second PET scan and EBUS. Patient 4 was not able to undergo any study procedures. Patient 9 refused the second EBUS. The mean PFS and overall survival (OS) of the included patients were 96 and 222 days, respectively. Patient 10 had early-stage disease and, instead of a second PET-CT, underwent a lobectomy after two cycles of neoadjuvant PD-1 checkpoint inhibition; a complete pathological response was found in the resection specimen of this patient.

^{18}F-FDG-PET tracer uptake dynamics in tumor tissue.

In 5 out of 10 patients, both a baseline and a sequential ^{18}F-FDG-PET was obtained 7–14 days after the first nivolumab was administered. The baseline and dynamics of tracer uptake in tumor tissue are shown in Table S3. All patients showed an increase in SUVpeak and all but one in SUVmax; the degree of the increase was strongly correlated with clinical outcome, with more pronounced increases in patients with sorter OS (Figure 1a). In patients 2 and 9, a marginal decrease in TLG was found, whereas patients 5, 6, and 7 showed an increase in TLG of 21%, 119%, and 171%, respectively (Table S3, Figure 1b). The percentages of increase in TLG, SUVmax, and SUVpeak were negatively correlated with PFS and OS. Delta SUVmax and SUVpeak of all lesions showed a strong correlation with PFS and OS (r SUVmax $r = -0.72/-0.89$ and r SUVpeak $r = -0.69/-0.84$, respectively; for OS correlations, see Figure 1A) On-treatment TLG change showed a strong and significant correlation with OS $r = -0.93$ ($p = 0.022$, Figure 1B). The PFS had a non-significant correlation of -0.81 ($p = 0.097$) with TLG.

T-cell profiles in TDLN and PBMC in relation to response and clinical outcome

PBMC and TDLN cells of seven patients were analyzed by FACS for T-cell subset frequencies and activation state. Five of these patients underwent both an EBUS before and 7–14 days after the first administration of PD-1 checkpoint inhibitor (Table S2). Baseline and on-treatment changes in the T-cell profile were related to response to PD-1 blockade (Figure 2). Of note, the inclusion of only two responders undergoing sequential EBUS-FNA precluded meaningful statistical analysis of TDLN T-cell profiles in progressors versus responders. Nevertheless, some interesting observations pointed to the particular utility of TDLN-based T-cell parameters for outcome prediction of PD-1 blockade.

No obvious differences in T-cell profiles were apparent between responders and progressors at baseline, neither in PBMC nor in TDLN, with the possible exception of frequencies of PD-1^{hi} CD8$^+$ T cells and PD-1^{hi} Tregs, with higher frequencies of both subsets in TDLN of both responders as compared to the three progressors (Figure 2a).

Whereas no clear differences in dynamics of the T-cell parameters from baseline to day 7–14 post PD-1 blockade were found between responders and progressors in PBMC, some clear and consistent differences became apparent
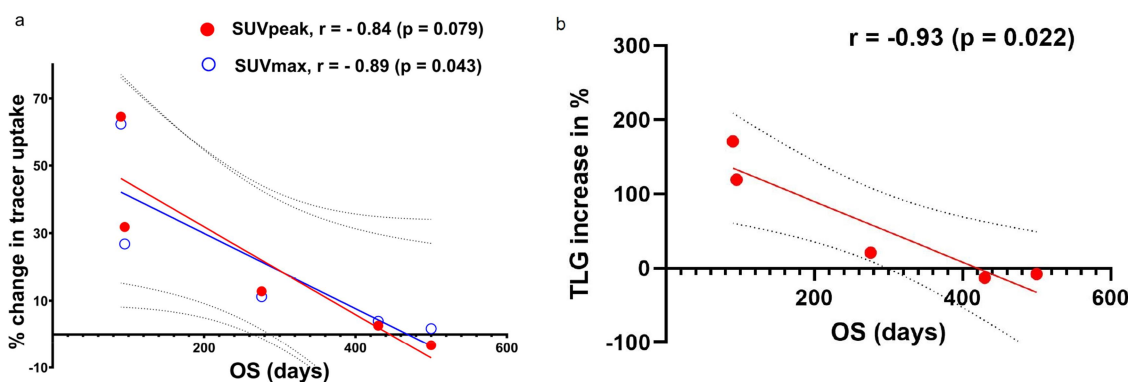

Figure 1. Relation tracer uptake and overall survival. Note: Percentage of change of tracer uptake in all tumor lesions from baseline to 7–14 days after the initiation of anti-PD-1 treatment. (a) An increase in SUVmax and SUVpeak shows a reverse correlation with OS. (b) An increase in TLG shows a significant reverse correlation with OS.
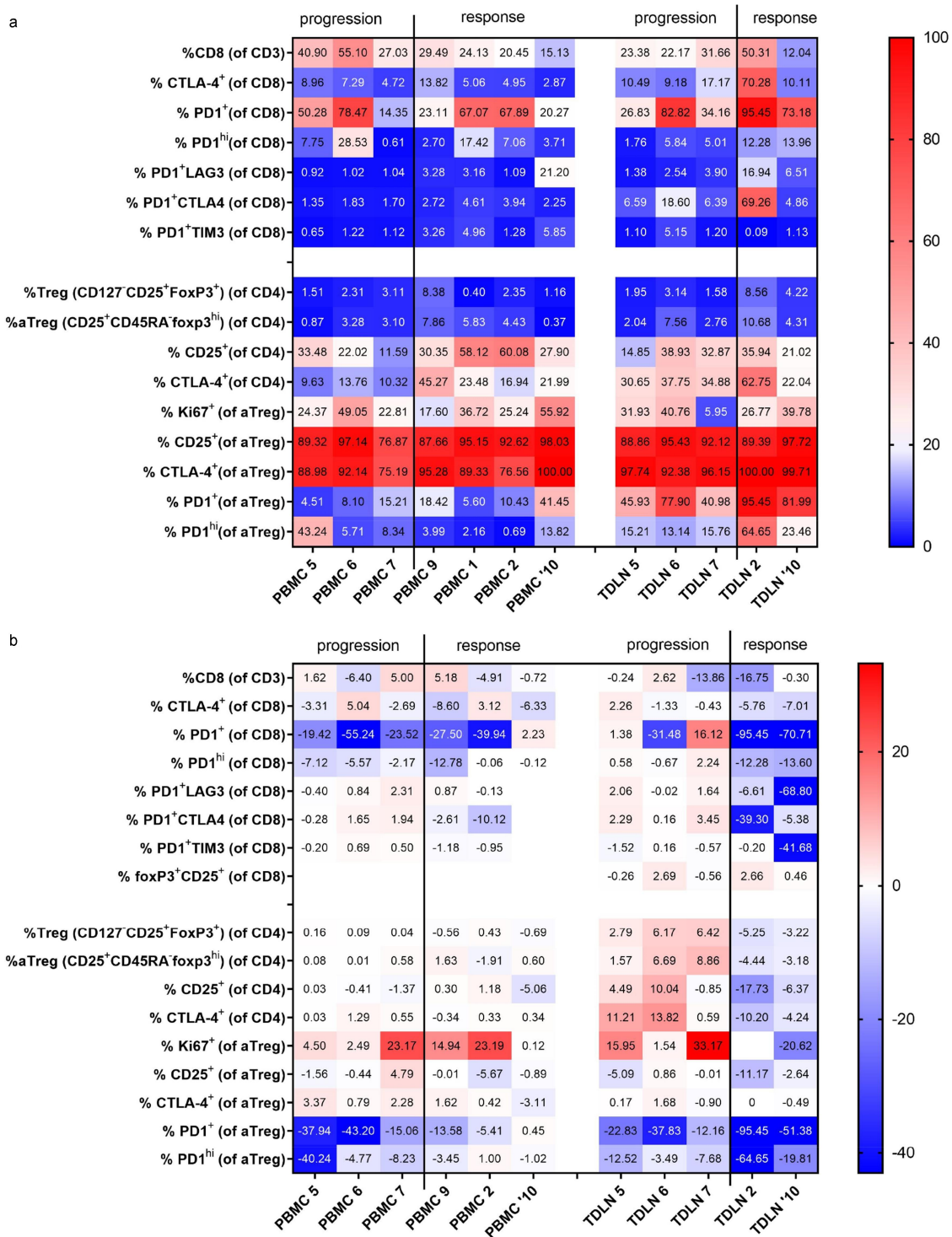
Figure 2. Heat map of T-cell subsets in PMBC and TDLN. Note: The patient group was divided into patients with progression and patients who had a favorable response to immunotherapy. (a) Percentages of T-cell subsets at baseline. (b) Increase or decrease in the percentage of T-cell subsets from baseline at 7–14 days

between these groups in the TDLN samples (Figure 2b). Most notably, there was an increase in Treg frequencies in the progressors, which was mainly driven by activated Tregs (aTregs) with coinciding elevations in Ki67. This was accompanied by increased rates of CD25$^+$ and CTLA4$^+$ CD4$^+$ T cells. In contrast, all these parameters decreased in the TDLN of responders. Rates of PD-1-expressing Tregs (both with high and intermediate levels) decreased more profoundly in responders than progressors.

In addition, frequencies of PD-1 (both intermediate and high) expressing CD8$^+$ T cells decreased consistently in responders but remained stable in progressors. Similarly, co-expression of the other immune checkpoints CTLA4, LAG3, and TIM3 on PD-1$^+$ CD8$^+$ T cells also decreased in both responders but failed to do so in all three progressors, signaling a drop in exhausted CD8$^+$ T cell rates in the former and stable frequencies of exhausted CD8$^+$ T cells in the latter (Figure 2b.).
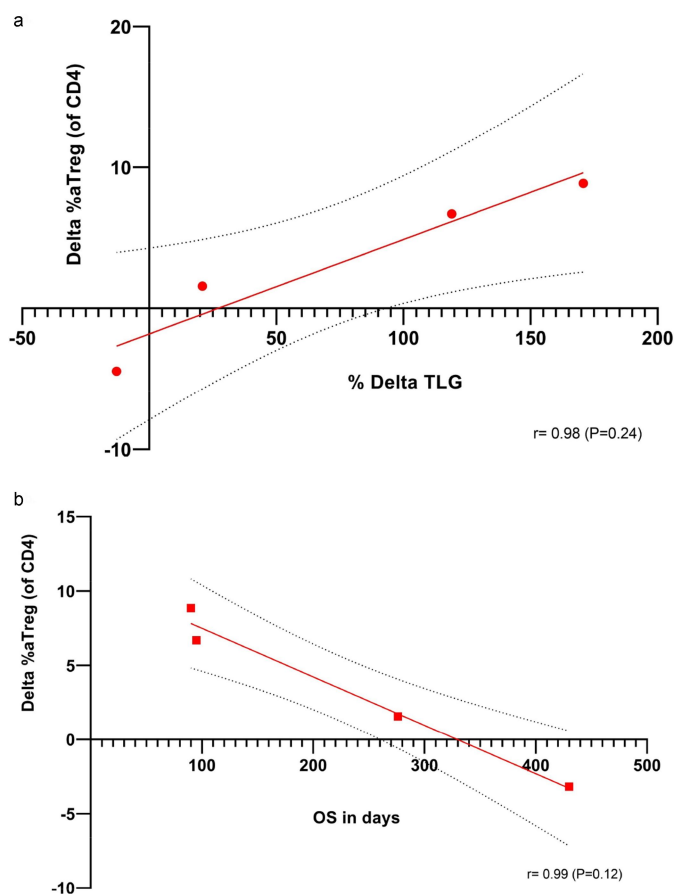
Figure 3. Relation delta aTreg and delta TLG or overall survival. Note: Percentage of aTregs (of CD4) at baseline minus percentage of aTregs (of CD4) at 7–14 days after initiation of PD-1 inhibition correlated with (a) Change in TLG in percentage at baseline and at 7–14 days after the initiation of PD-1 inhibition. (b) OS.

^{18}F-FDG-PET tumor leasion glycolysis dynamics correlated with TDLN immune subsets.

Earlier research showed a correlation between FDG uptake and the presence of Tregs in the tumor microenvironment of NSCLC.[10] In our data set, the FDG uptake in SUVmax of the hottest leasion was highest in patient 2; interestingly, this patient had the highest percentage of aTregs and CD8 cells in TDLN (Table S2, Figure 2). The total uptake of FDG (TLG) was correlated with the increase in aTregs rates in TDLN upon PD-1 blockade (Figure 3a), which in turn showed a near-perfect reverse correlation with overall survival (Figure 3b). Both correlations failed to reach significance due to the small number of available data points (*n* = 4).

Discussion

The anti-tumor immune response is complex and not completely understood. As a result of this complexity, the perfect predictive biomarker for immune checkpoint blockade has not yet been identified. We studied T-cell profile dynamics and changes in FDG uptake shortly (7–14 days) after treatment initiation with a PD-1 checkpoint inhibitor in patients with early-stage or advanced NSCLC, in correlation with each other and clinical outcome.

Pre- and early on-treatment T-cell profiling was performed both in peripheral blood and in TDLN from patients undergoing PD-1 blockade. Remarkably, distinct on-treatment changes in CD8^{+} T cell and Treg profiles were observed in the TDLN rather than in the peripheral blood of progressors versus responders. This observation is in line with the recently reported essential role of TDLN in the efficacy of PD-(L)1 checkpoint inhibitor therapy.[5,11] In this light, TDLN should most decidedly be explored for their biomarker potential. To the best of our knowledge, our study is the first to analyze the change in T-cell subset composition of the TDLN *in vivo* after the treatment initiation with an anti-PD-1 checkpoint inhibitor. Here, we report that an increase in Treg frequencies in the TDLN might be a sign of anti-PD-1 checkpoint inhibitor resistance as it was selectively observed in progressors. Immune suppressive Tregs and potentially immune suppressed/exhausted CD8^{+} T cells declined in the responding patients. In addition, an increase in ^{18}F-FDG tracer uptake, expresses as TLG, 7–14 days after the treatment initiation also strongly correlated with treatment resistance. These findings might contribute to a better understanding of the mechanisms of treatment response or resistance and the role of the TDLN field.

Exhausted CD8 T-cells, often described as PD-1^{+}/PD-1^{hi} with co-expression of other immune checkpoints such as LAG3 and TIM3, are immune suppressed with a decreased pro-inflammatory cytokine production and impaired cytotoxicity.[12] We found T cells with this particular PD-1^{+} phenotype to decrease in frequency in the TDLN of responders to PD-1 blockade, whereas they remained stable in on-treatment progressors. Protracted PD-1 occupancy on T cells upon administration of blocking PD-1 antibodies, interfering with subsequent PD-1 staining, was previously reported and suggested as a possible biomarker for efficacy.[13] In this context, it is of interest that we observed profound decreases in detectable PD-1-expressing CD8^{+} T cells and Tregs in responders, but not (or to a lesser degree) in progressors. This could perhaps indicate rapid upregulation of newly expressed PD-1 molecules at the T-cell surface and thereby maintained PD-1 mediated immune suppression in patients who did not respond to treatment. Previous studies also reported that an IFNγ response induced by PD-1 blockade could lead to PD-1 downregulation.[14] Using serum CXCL10 levels as a measure of IFNγ response, we could find no relationship with (on-treatment) PD-1 expression levels nor with response (data not shown). Interestingly, there was no distinct change in rates of effector T-cells or T-helper cells upon PD-1 blockade. Rather, our data suggest that the disappearance of an immune suppressive microenvironment in the TDLN is more predictive of a favorable response and outcome than an increase in rates of effector T-cells.

Earlier *in-vitro* studies have demonstrated that PD-1-blocking antibodies could enhance the suppressive function of peripheral Tregs[15]. Also, in the tumor microenvironment (TME), the activation and expansion of tumor-infiltrating Tregs after PD-1 blockade have been suggested as a mechanism of resistance to anti-PD-1 checkpoint inhibitors. This resistance would be caused by the balance of PD-1 expression on CD8^{+} T cells and Tregs leaning too much to the Tregs, resulting in

stronger activation of Tregs compared to CD8^{+} T cells.[16] Tregs in the TME that express PD-1 have been linked to rapidly progressive disease or hyper progression after the initiation of anti-PD-1 checkpoint inhibition.[17] These results and our findings combined suggest that the dynamic changes reported among T-cell subsets in the TME upon PD-1 blockade reflect similar changes in the TDLN. In this regard, it is also of interest that responding patients had higher rates of PD-1^{hi}CD8^{+} T cells in their TDLN at baseline. We would propose that these T cells might be the phenotypic and functional equivalent of the so-called PD-1[T] T cells, enriched for tumor-specific T cells, which were recently identified in the TME of NSCLC (and more specifically in tertiary lymphoid structures) and shown to be predictive for outcome of PD-1 blockade.[18] Interestingly, similarly elevated frequencies of PD-1^{hi} Tregs in responder TDLN at baseline apparently resulted in decreased Treg rates in the TDLN, and perhaps eventually also in the TME, after the initiation of PD-1 blockade (see Figure 2a).

Next to the increase in Tregs in TDLNs after the treatment initiation, our findings indicate that an increase in ^{18}F-FDG tumor uptake expressed as TLG was correlated with unfavorable outcomes. These results are comparable with observations in a previous study in which patients with advanced NSCLC had a follow-up ^{18}F-FDG-PET/CT after 4 months. A decrease in TLG was observed in patients with clinical benefits.[19] Our data show the same pattern already at 7–14 days after the treatment initiation. In addition, in patients with HNSCC who underwent neoadjuvant immunotherapy, a decrease in TLG at 4 weeks compared to baseline correlated with pathological response in the resected tumor.[3] It is unclear whether these early changes in ^{18}F-FDG uptake are solely due to tumor growth. Accumulation of ^{18}F-FDG is also high in macrophages, neutrophils and lymphocytes.[20] A correlation between ^{18}F-FDG uptake in NSCLC an immune infiltrate characterized by PD-1^{+} CD8 T cells and Foxp3^{+} regulatory T cells (Tregs) has been described as well.[10] Additionally, next to the changes in frequencies, also changes in T-cell metabolism after PD-1 blockade could influence the changes in FDG uptake[21]. These observations correspond to our finding that the patient with the highest tumor tracer uptake at baseline had the highest percentage of CD8 T cells and aTregs in the TDLN, as this might reflect the immune cell composition of the tumor. The patient from our study who was treated with neoadjuvant pembrolizumab had a complete pathological response. While this patient did not undergo an on-treatment ^{18}F-FDG-PET, the dynamic changes in Treg and PD-1^{+}CD8^{+} T-cell frequencies were comparable to the other patient with clinical benefit, i.e. they decreased. PD-1 checkpoint inhibition can result in higher FDG uptake shortly after the anti-PD-1 administration, hypothesized to be due to the influx of immune cells.[10] Interestingly, our data indicate that an increase in tracer uptake is correlated with an increase in Tregs in the TDLN, but not of effector T cells. This finding corresponds to the results from a study in gastric cancer, where SUVmax had a higher correlation with Foxp3^{+} T lymphocyte counts than with CD3^{+} lymphocyte counts.[22] Unfortunately, on-treatment tumor biopsies were not available in our cohort. As a result, we were not able to assess which cells, i.e. tumor or immune cells, were most likely responsible for the observed changes in FDG uptake in the tumor lesions. Nevertheless, our findings suggest that rather than an effector T-cell influx and expansion, the increased FDG uptake may be due to intensified tumor metabolism/ growth as a response to increased immune suppression mediated, or at least marked, by increased Treg rates.

Our data demonstrate the feasibility of repeated simultaneous measurements, at a brief interval from the start of treatment, of immune subsets in TDLN and peripheral blood and of PET imaging parameters. EBUS-FNA of TDLN provides the means for repeated loco-regional immune measurements, whereas repeated histological tumor biopsies are often not feasible in patients with NSCLC. The results of this study indicate a potential predictive value of combined early FDG-PET and assessment of T-cell dynamics in the TDLN shortly after the initiation of immunotherapy.

The obvious weak point of our study is the very small sample size, which results in conclusions that are hypothesis-generating at most. Therefore, more research in larger cohorts is warranted since the indications and application of checkpoint inhibitor therapy are still expanding. While FNA of the TDLN using EBUS is a low-risk procedure, it still is invasive. Because of this, blood-derived biomarkers are preferred from a patient perspective. Hypothetically, screening the blood for exosomes that might be responsible for reprogramming of the TDLN to a pre-metastatic niche might give a surrogate signal of the local immune response.[23,24]

A potential application of early response monitoring can be in the neoadjuvant setting, where the potential of immunotherapy in NSCLC has recently been demonstrated.[25] In this setting, an early read-out of treatment failures would be very valuable since time to surgery should be as short as possible and an ineffective and possibly toxic neoadjuvant treatment regimen should be discontinued. Additionally, an early read-out of the immune environment of the TDLN could differentiate pseudo-progression from actual progression and might guide clinicians in their treatment decisions. At the same time, a strong local immune response in TDLN might represent a systemic T-cell immunity that mediates the so-called abscopal effect such as observed in local ablation or radiotherapies.

In conclusion, this is the first clinical study in which changes in frequencies in TDLN shortly after PD-1 checkpoint inhibition were correlated with response in PFS, OS, and nuclear imaging. An increase in aTreg subsets seems to be predictive of an unfavorable treatment response and clinical outcome. Activation or expansion of effector subsets like CD8 effector T-cells did not differentiate between responders and non-responders in this study. An increase in TLG on an early on-treatment ^{18}F-FDG pet-scan showed a correlation with aTreg dynamics in TDLN and clinical outcome. These findings warrant further validation and exploration in a larger cohort of patients, including in the neoadjuvant setting.

Disclosure statement

Funding

Data availablity satatement

The authors confirm that the data supporting the findings of this study are available within the article and its supplementary materials.

References

1. Hendriks LE, Kerr KM, Menis J, Mok TS, Nestle U, Passaro A, Peters S, Planchard D, Smit EF, Solomon BJ, et al. Non-oncogene-addicted metastatic non-small-cell lung cancer: eSMO clinical practice guideline for diagnosis, treatment and follow-up. Ann Oncol. 2023:358–376. doi:10.1016/j.annonc.2022.12.013

2. Borm FJ, Smit J, Oprea-Lager DE, Wondergem M, Haanen JBAG, Smit EF, de Langen AJ. Response prediction and evaluation using PET in patients with solid tumors treated with immunotherapy. Cancers (Basel). 2021;13:3083. doi:10.3390/cancers13123083.

3. Vos JL, Zuur CL, Smit LA, de Boer JP, Al-Mamgani A, van den Brekel MWM, Haanen JBAG, Vogel WV. [(18)f]FDG-PET accurately identifies pathological response early upon neoadjuvant immune checkpoint blockade in head and neck squamous cell carcinoma. Eur J Nucl Med Mol Imaging. 2021;49:2010–2022. doi:10.1007/s00259-021-05610-x.

4. Munn DH, Mellor AL. The tumor-draining lymph node as an immune-privileged site. Immunol Rev. 2006;213:146–158. doi:10.1111/j.1600-065X.2006.00444.x.

5. van Pul KM, Fransen MF, van de Ven R, de Gruijl TD. Immunotherapy goes local: the central role of lymph nodes in driving tumor infiltration and efficacy. Front Immunol. 2021;12:643291. doi:10.3389/fimmu.2021.643291.

6. Bugalho A, Martins C, Silva Z, Nunes G, Mendes AS, Ferreira I, Videira PA. Immature myeloid cells and tolerogenic cytokine profile in lung adenocarcinoma metastatic lymph nodes assessed by endobronchial ultrasound. Tumour Biol. 2016;37:953–961. doi:10.1007/s13277-015-3885-1.

7. Murthy V, Katzman DP, Tsay J-CJ, Bessich JL, Michaud GC, Rafeq S, Minehart J. Tumor-draining lymph nodes demonstrate a suppressive immunophenotype in patients with non-small cell lung cancer assessed by endobronchial ultrasound-guided transbronchial needle aspiration: a pilot study. Lung Cancer. 2019;137:94–99. doi:10.1016/j.lungcan.2019.08.008.

8. van de Ven R, Niemeijer ALN, Stam AGM, Hashemi SMS, Slockers CG, Daniels JM, Thunnissen E, Smit EF, de Gruijl TD, de Langen AJ. High PD-1 expression on regulatory and effector T-cells in lung cancer draining lymph nodes. ERJ Open Res. 2017;3:00110–2016. doi:10.1183/23120541.00110-2016.

9. Lammertsma R, Oyen WJG, Boellaard AA, Spreeuwenberg MD, Smit EF, Hoekstra OS, Lammertsma AA. Reproducibility of tumor perfusion measurements using 15O-labeled water and PET. J Nucl Med. 2008;49:1763–1768. doi:10.2967/jnumed.108.053454.

10. Wang Y, Zhao N, Wu Z, Pan N, Shen X, Liu T, Wei F, You J, Xu W, Ren X. New insight on the correlation of metabolic status on (18) F-FDG PET/CT with immune marker expression in patients with non-small cell lung cancer. Eur J Nucl Med Mol Imaging. 2020;47:1127–1136. doi:10.1007/s00259-019-04500-7.

11. Dammeijer F, van Gulijk M, Mulder EE, Lukkes M, Klaase L, van den Bosch T, van Nimwegen M, Lau SP, Latupeirissa K, Schetters S, et al. The PD-1/PD-L1-checkpoint restrains T cell immunity in tumor-draining lymph nodes. Cancer Cell. 2020;38:685–700.e688. doi:10.1016/j.ccell.2020.09.001.

12. Wherry EJ, Kurachi M. Molecular and cellular insights into T cell exhaustion. Nat Rev Immunol. 2015;15:486–499. doi:10.1038/nri3862.

13. Brahmer JR, Drake CG, Wollner I, Powderly JD, Picus J, Sharfman WH, Stankevich E, Pons A, Salay TM, McMiller TL, et al. Phase I study of single-agent anti–programmed death-1 (MDX-1106) in refractory solid tumors: safety, clinical activity, pharmacodynamics, and immunologic correlates. J Clin Oncol. 2010;28:3167–3175. doi:10.1200/jco.2009.26.7609.

14. Ding G, Shen T, Yan C, Zhang M, Wu Z, Cao L. IFN-γ down-regulates the PD-1 expression and assist nivolumab in PD-1-blockade effect on CD8+ T-lymphocytes in pancreatic cancer. BMC Cancer. 2019;19:1053. doi:10.1186/s12885-019-6145-8.

15. Woods DM, Ramakrishnan R, Laino AS, Berglund A, Walton K, Betts BC, Weber JS. Decreased suppression and increased phosphorylated STAT3 in regulatory T cells are associated with benefit from adjuvant PD-1 blockade in resected metastatic melanoma. Clin Cancer Res. 2018;24:6236–6247. doi:10.1158/1078-0432.Ccr-18-1100.

16. Kumagai S, Togashi Y, Kamada T, Sugiyama E, Nishinakamura H, Takeuchi Y, Vitaly K, Itahashi K, Maeda Y, Matsui S, et al. The PD-1 expression balance between effector and regulatory T cells predicts the clinical efficacy of PD-1 blockade therapies. Nat Immunol. 2020;21:1346–1358. doi:10.1038/s41590-020-0769-3.

17. Kamada T, Togashi Y, Tay C, Ha D, Sasaki A, Nakamura Y, Sato E, Fukuoka S, Tada Y, Tanaka A, et al. PD-1 + regulatory T cells amplified by PD-1 blockade promote hyperprogression of cancer. Proc Natl Acad Sci U S A. 2019;116:9999–10008. doi:10.1073/pnas.1822001116.

18. Hummelink K, van der Noort V, Muller M, Schouten RD, Lalezari F, Peters D, Theelen WSME, Koelzer VH, Mertz KD, Zippelius A, et al. PD-1T TILs as a predictive biomarker for clinical benefit to PD-1 blockade in patients with advanced NSCLC. Clin Cancer Res. 2022:4893–4906. doi:10.1158/1078-0432.Ccr-22-0992

19. Ferrari C, Santo G, Merenda N, Branca A, Mammucci P, Pizzutilo P, Gadaleta CD, Rubini G. Immune checkpoint inhibitors in advanced NSCLC: [(18)F]FDG PET/CT as a troubleshooter in treatment response. Diagnostics (Basel). 2021;11. doi:10.3390/diagnostics11091681.

20. Jones HA, Cadwallader KA, White JF, Uddin M, Peters AM, Chilvers ER. Dissociation between respiratory burst activity and deoxyglucose uptake in human neutrophil granulocytes: implications for interpretation of (18)F-FDG PET images. J Nucl Med. 2002;43:652–657.

21. Patsoukis N, Bardhan K, Chatterjee P, Sari D, Liu B, Bell LN, Karoly ED, Freeman GJ, Petkova V, Seth P, et al. PD-1 alters T-cell metabolic reprogramming by inhibiting glycolysis and promoting lipolysis and fatty acid oxidation. Nat Commun. 2015;6:6692. doi:10.1038/ncomms7692.

22. Lee S, Choi S, Kim SY, Yun MJ, Kim H-I. Potential utility of FDG PET-CT as a non-invasive tool for monitoring local immune responses. J Gastric Cancer. 2017;17:384–393. doi:10.5230/jgc.2017.17.e43.

23. Poggio M, Hu T, Pai C-C, Chu B, Belair CD, Chang A, Montabana E, Lang UE, Fu Q, Fong L, et al. Suppression of exosomal PD-L1 induces systemic anti-tumor immunity and memory. Cell. 2019;177:414–427.e413. doi:10.1016/j.cell.2019.02.016.

24. Zhang Z, Jin W, Xu K, Zheng X, Zhou Y, Luo M, Yan C, Zheng X, Jin E. Blood exosome PD-L1 is associated with PD-L1 expression measured by immunohistochemistry, and lymph node metastasis in lung cancer. Tissue Cell. 2022;79:101941. doi:10.1016/j.tice.2022.101941.

25. Forde PM, Spicer J, Lu S, Provencio M, Mitsudomi T, Awad MM, Felip E, Broderick SR, Brahmer JR, Swanson SJ, et al. Neoadjuvant nivolumab plus chemotherapy in resectable lung cancer. N Engl J Med. 2022;386:1973–1985. doi:10.1056/NEJMoa2202170.